CLIMATE VARIABILITY OF A COUPLED OCEAN–ATMOSPHERE–LAND SURFACE MODEL: IMPLICATION FOR THE DETECTION OF GLOBAL WARMING

SYUKURO MANABE AND RONALD J. STOUFFER

Printed in the United States of America
Reprinted from BULLETIN OF THE AMERICAN METEOROLOGICAL SOCIETY
Vol. 78, No. 6, June 1997

Climate Variability of a Coupled Ocean–Atmosphere–Land Surface Model: Implication for the Detection of Global Warming*

Walter Orr Roberts Lecture

Syukuro Manabe and Ronald J. Stouffer
Geophysical Fluid Dynamics Laboratory/NOAA, Princeton University, Princeton, New Jersey

ABSTRACT

This lecture evaluates the low-frequency variability of surface air temperature that was obtained from a 1000-yr integration of a coupled ocean–atmosphere–land surface model. The model simulates reasonably well the variability of local and global mean surface air temperature (SAT) at decadal timescales. The physical mechanisms responsible for this variability are explored. Based upon an analysis of the time series of the simulated global mean SAT, it is indicated that the warming trend of ~0.5°C century^{-1} since the end of the last century was not generated internally through the interaction among the atmosphere, ocean, and land surface. Instead, it appears to have been induced by a sustained change in the thermal forcing such as that resulting from changes in atmospheric greenhouse gas concentration, solar irradiance, and aerosol loading.

1. Introduction

One of the emerging tools for the study of climate variability is a coupled ocean–atmosphere–land surface model in which a general circulation model of the atmosphere is coupled to a general circulation model of the oceans and a land model representing the heat and water budget of the continental surface. Referring to the climate variability simulated by a 1000-yr integration of a coupled model, this lecture attempts to answer the following questions.

1) How well does the coupled model simulate the decadal variability of local and globally averaged surface air temperature?
2) What are the physical mechanisms responsible for this decadal variability?
3) Have we distinguished the thermally forced global warming from internally generated natural variability?

Syukuro Manabe

Figure 1 illustrates the time series of globally averaged, annual mean surface temperature (Jones and Wigley 1991). In addition to the general warming trend, which began around the turn of the twentieth century, this time series exhibits large fluctuations of the global mean temperature, at not only interannual but also multidecadal timescales. Here we evaluate this time series based upon the results from several numerical experiments which were performed at NOAA's Geophysical Fluid Dynamics Laboratory.

For a more detailed description and evaluation of the simulated variability of surface air temperature, refer to the studies by Manabe and Stouffer (1996) and Hall and Manabe (1997). The model

*This lecture was presented at the 77th AMS Annual Meeting in Long Beach, California, on 5 February 1997.

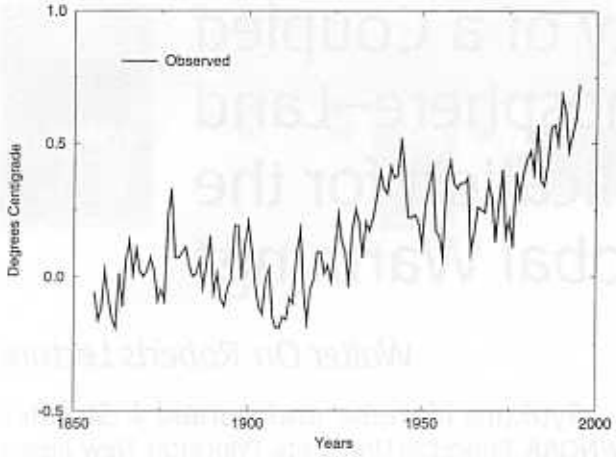

FIG. 1. Time series of globally averaged, annual mean surface air temperature anomalies (i.e., the departures from the 1880–1920 base-period means) obtained by Jones and Wigley (1991).

assessment of the observed warming trend was made earlier by Stouffer et al. (1994).

2. Numerical experiment

The coupled model used here consists of general circulation models (GCMs) of the atmosphere and oceans with sea ice and a simple model of land surface that includes the budgets of heat and water (Fig. 2). It is a global model with realistic geography. The atmospheric GCM includes the seasonal variation of insolation and predicted cloud cover. It has nine vertical finite-difference levels. The horizontal distributions of predicted variables are represented by spherical harmonics (15 associated Legendre functions for each of 15 Fourier components) and by corresponding grid points. The oceanic GCM uses a finite-difference technique with a regular grid system that has horizontal spacing of 4.5° latitude × 3.75° longitude and 12 vertical levels.

For economy of computer time, the coupled model described above has relatively low computational resolution and contains relatively simple parameterizations of various physical processes. Despite its simplicity, the coupled model successfully reproduces the standard deviation of surface air temperature variability as described in this following section, encouraging us to use it for the study of climate variability.

We conducted a 1000-yr time integration of the coupled model described above. The initial conditions for the control experiment have realistic seasonal and geographical distributions of sea surface temperature, surface salinity, and sea ice, with which both the atmospheric and oceanic model states are nearly in equilibrium. When the time integration of the model starts from this initial condition, the model climate drifts towards its own equilibrium state, which differs from the realistic initial condition described above (e.g., Manabe and Stouffer 1988). To reduce this drift that results from the imperfection of a model, the fluxes of heat and water obtained from the atmospheric component of the coupled model are modified by given amounts before they are imposed at the oceanic surface. Because the adjustments are determined before the time integration of the coupled model, and are not correlated to the transient surface anomalies of temperature and salinity that can develop during the integration, they are unlikely to either systematically amplify or damp the anomalies. The adjustments do not eliminate the shortcomings of the model physics, which could distort the simulated transients. But the adjustments do prevent the rapid drift of the model state from the realistic initial condition, which could seriously distort the results of a numerical experiment.

Owing to the flux adjustment and initialization technique described above, the climate of the coupled model remains realistic during the 1000-yr period. Thus, the coverages of sea ice and snow, which control the albedo feedback process, remain realistic. A rapid, initial change in the intensity of the thermohaline circulation is avoided, thereby preventing the artificial drift of water mass structure that distorts the multidecadal variability of climate

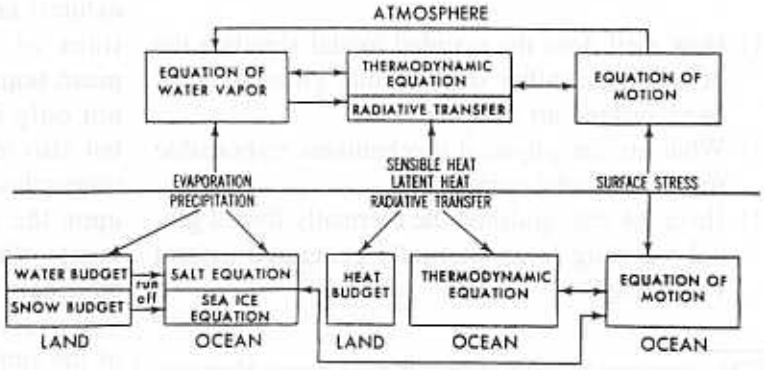

FIG. 2. Box diagram that illustrates the structure of the coupled ocean–atmosphere–land surface model.

in the coupled system. We believe that the technique of flux adjustment described above is an attractive alternative, pending the completion of the more realistic models of the coupled system in the future.

To identify the role of the oceans in the low-frequency fluctuation of climate, long-term integrations of two different models (Fig. 3) are compared with each other. The first model, the "coupled model" described above, is constructed by combining a general circulation model of the atmosphere with that of the oceans. The second model, the "mixed layer model" is made by combining the general circulation model of the atmosphere with a very simple mixed layer ocean model that is vertically well-mixed layer of water with uniform thickness of 50 m. To mimic the convergence of horizontal heat transport by ocean currents, heat flux is prescribed at the bottom of the mixed layer ocean depending on season and geography. The annual cycle of heat flux, however, repeats itself exactly and does not change from one year to the next. By comparing long-term integration of these two models, we hope to investigate how the temporal variations of the transport and storage of heat in the oceans affect the variability of climate.

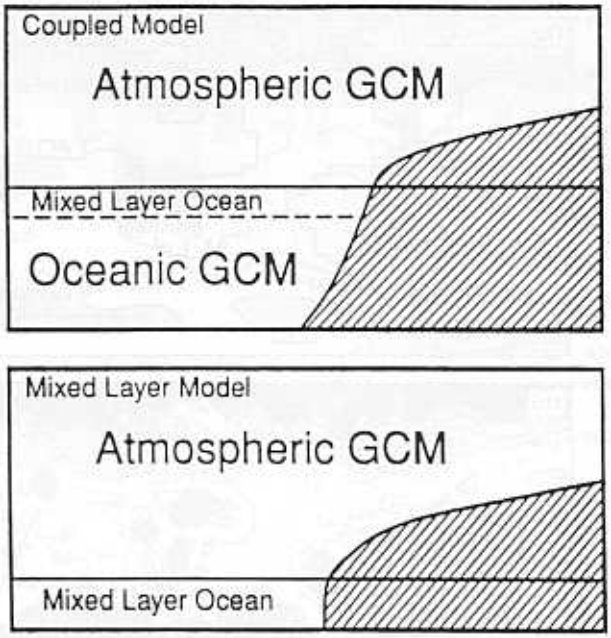

FIG. 3. Two models used: (a) coupled model, (b) mixed layer model.

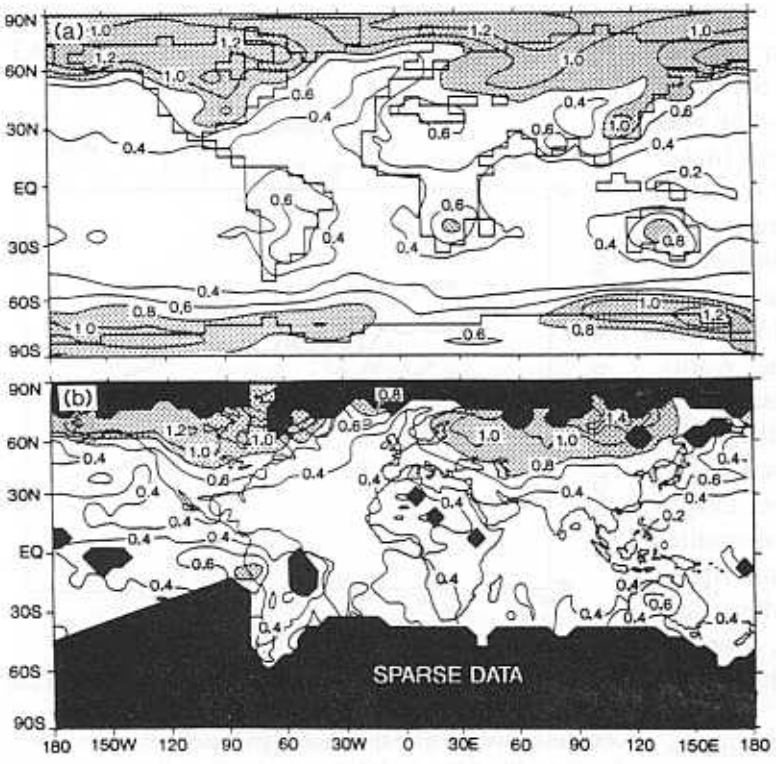

FIG. 4. Geographical distributions of the standard deviation of annual mean SAT anomaly (°C): (a) coupled model, (b) observed (Jones and Wigley 1991). To determine SAT distribution, Jones and Wigley complemented SAT by SST data. Thus, observed variability of annual mean SAT (b) may be underestimated.

3. Local variability

To examine the local variability of surface air temperature on interannual and decadal timescales, the geographical distributions of the standard deviation of annual and 5-yr mean surface air temperature (SAT) of the coupled model are illustrated in Figs. 4 and 5 and are compared with the observed distributions. These figures indicate that, with the exception of the eastern tropical Pacific where the magnitude of sea surface temperature (SST) variability associated with the Southern Oscillation is large, the coupled model simulates reasonably well the observed variability of local SAT at interannual and decadal timescales. The simulated variability is usually larger over continents than oceans in agreement with observations. This land–sea contrast in variability holds not only for the annual but also for the decadal and multidecadal timescales.

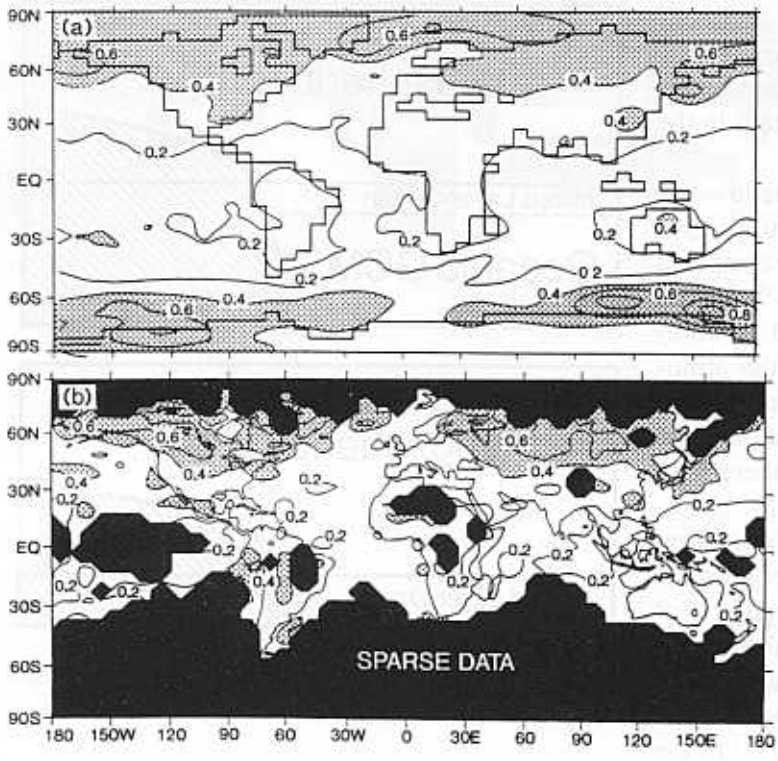

FIG. 5. Geographical distributions of the standard deviation of 5-yr mean SAT anomaly (°C): (a) coupled model, (b) observed (Jones and Wigley 1991).

As Fig. 6 indicates, the year-to-century part of the simulated spectrum of monthly mean SAT over continents in middle latitudes is almost white with a slight downward bend at the frequencies higher than 1 cycle yr^{-1}. The power of the SAT spectrum over most of the oceans, however, increases very gradually with decreasing frequency as influenced by the thermal inertia of underlying oceans and approaches the power of the continental spectrum at decadal and longer timescales. In other words, local SAT variability over continents is larger than those over oceans, at not only interannual but also decadal and longer timescales. We believe that this difference results mainly from the slower evaporative damping of surface temperature anomalies over continents as compared with oceans. At the oceanic surface of low and midlatitudes where saturation vapor pressure is relatively high, evaporative ventilation is very effective in reducing surface temperature anomalies.

In the midoceanic regions of the midlatitudes, the spectrum of SST anomalies of both coupled and mixed layer models may be characterized as a red noise spectrum indicative of the first order Markov process (Fig. 7). This result appears to be consistent with the linear stochastic theory of Hasselmann (1976), which regards the observed variation of SST anomaly as the red noise response to the white noise forcing by synoptic-scale disturbances in the atmosphere. At the timescales that are much longer than the duration of a synoptic-scale disturbance, the thermal forcing of the atmosphere upon oceanic surface may be characterized as white noise. Hasselmann (1976) noted that, at relatively high frequencies, the mixed layer ocean with large thermal inertia serves as the integrator of the white noise forcing of the atmosphere, yielding a power spectrum for SST that is inversely proportional to the square of frequency. On the other hand, at low frequency, the mixed layer is in near thermal equilibrium with the white noise atmospheric forcing, yielding the SST spectrum, which is also white. Thus, the power spectrum of SST time series over the whole frequency range could be characterized as red noise. The red noise SST anomalies, in turn, affect SAT

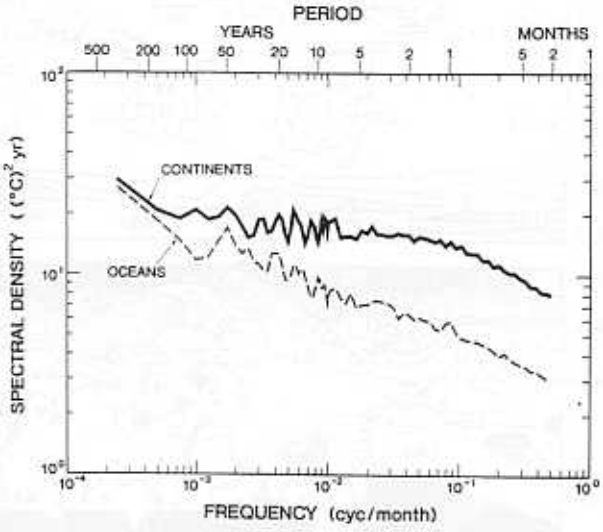

FIG. 6. Power spectra of monthly mean SAT anomaly of the coupled model. Continental and oceanic spectra, respectively, are obtained by averaging the spectra of all grid points, which are located inside the 30°–60° latitude belt in the Northern Hemisphere. The spectra are the smoothed Fourier transform of the autocovariance function using a Tukey window with a maximum of 2400 (200 yr) lags. They are smoothed by the equally weighted averaging over the logarithmic (base 10) interval of 0.04 in frequency.

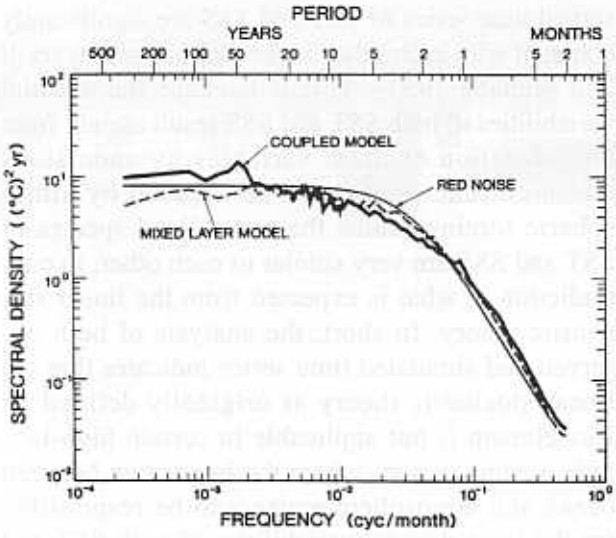

FIG. 7. Power spectra of monthly mean SST anomaly of the coupled and the mixed layer models. Both spectra are obtained by averaging the spectra of all grid points, which are located in the midoceanic boxes of the North Pacific (42.2°–28.9°N, 155.6°E–140.1°W) and North Atlantic (42.2°–28.9°N, 61.9°E–28.1°W). The specific details for computing these power spectra are contained in the caption of Fig. 6. The thin line is the least square fit of the red noise spectrum to the spectrum of SST from the coupled model (thick solid line).

anomalies directly above such that their spectral power increases gradually with decreasing frequency (Fig. 6).

Recently, Hall and Manabe (1997) analyzed the observed time series of SST and SSS (sea surface salinity) at the weather station "Papa" located in the northwestern North Pacific (51.8°N, 148.1°W). Both of these time series exhibit the red noise characteristic. The SSS spectrum is significantly redder than the SST spectrum, underscoring the weaker damping of SSS as compared with SST anomaly. It is expected that SST anomaly is reduced much faster than SSS anomaly because of the heat exchange of ocean–atmosphere interface through radiative, sensible, and latent heat fluxes. These results appear to be consistent with the linear stochastic theory of Hasselmann (1976).

Hasselmann's theory could also be applied to evaluate the temporal variation of continental surface temperature. Since the effective thermal inertia of the continental surface is small, the surface temperature is in equilibrium with the almost-white noise thermal forcing from the atmosphere, yielding an almost white noise power spectrum over a wide range of frequencies. The white noise fluctuation of surface temperature, in turn, closely interacts with the atmosphere mainly through boundary layer heat exchange, maintaining the almost-white noise SAT spectrum as described above (Fig. 6).

The applicability of the linear stochastic theory is reduced in certain subpolar regions of the model oceans where thermohaline circulation and associated convection often penetrate very deeply. These regions include the Nordic Seas, the Okhotsk Sea, and the circumpolar ocean of the Southern Hemisphere. In these regions of the coupled model, both SST and SAT are very persistent (Fig. 8), and their spectral densities at decadal and longer timescales are much larger than those of the mixed layer models (Fig. 9), due to the advection of SST by ocean currents in the coupled model. The difference in spectral densities underscores the important role that ocean circulation plays in enhancing the variabilities of both SAT and SST at these timescales. For example, the pronounced multidecadal oscillations of SST and SSS in the Greenland Sea of the coupled model are associated with fluctuations in the intensity of the East Greenland Current and convective activity in the Greenland Sea (Delworth et al. 1997). The Greenland Sea temperature and salinity variations are preceded by near-surface salinity variations in the Arctic through the East Greenland Current. These modeled salinity anomalies then propagate around the subpolar gyre into the Labrador Sea and the central North Atlantic in a manner similar to

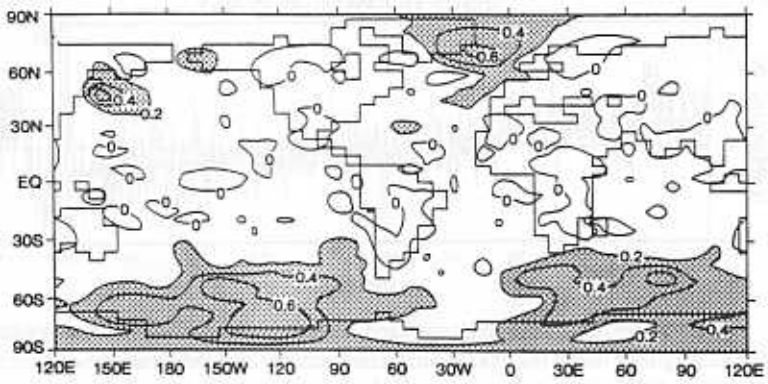

FIG. 8. Geographical distribution of autocorrelation coefficient (lag: 5 yr) for the time series of 5-yr mean SAT anomalies from the coupled model.

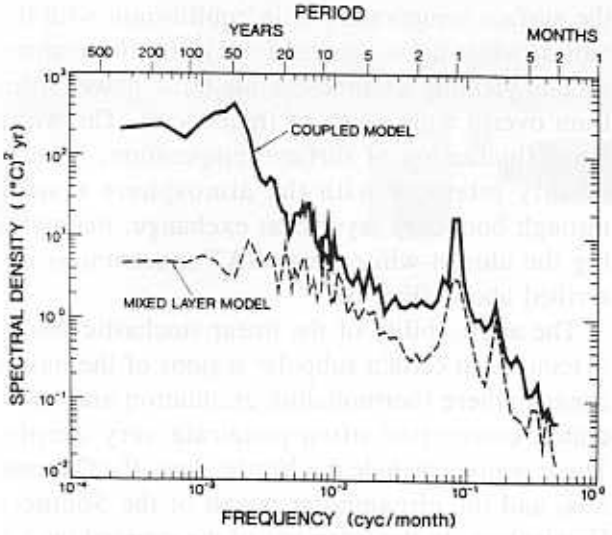

FIG. 9. Power spectra of monthly mean SST anomaly at 69.75°N, 22.5°W of the coupled (solid line) and mixed layer (dashed line) models. The specific details for computing these power spectra are contained in the caption of Fig. 6.

the "Great Salinity Anomaly." The cold SST anomalies in the Greenland Sea, in turn, induce the slight eastward shift of the Icelandic low, resulting in the weakening of southerly wind over the Nordic Seas. Thus, the East Greenland Current intensifies, further reducing SST in the Greenland Sea. The Greenland Sea Oscillation described here appears to interact and is coherent with the previously identified multidecadal fluctuation in the intensity of the North Atlantic thermohaline circulation of the coupled model (Delworth et al. 1993).

At the weather station "India" located in the northern North Atlantic (60.8°N, 20.6°W), the observed time series of SST and SSS are significantly coherent with each other at decadal timescales (Hall and Manabe 1997). This is because the decadal variabilities of both SST and SSS result mainly from the advection of these variables by anomalous ocean currents that could be induced by atmospheric forcing. Thus, the normalized spectra of SST and SSS are very similar to each other, in contradiction to what is expected from the linear stochastic theory. In short, the analysis of both observed and simulated time series indicates that the linear stochastic theory as originally defined by Hasselmann is not applicable in certain high-latitude oceanic regions where the interaction between ocean and atmosphere appears to be responsible for the large decadal variabilities of both SST and SSS.

4. Global variability

As discussed in the introduction, the detection of global warming has been an important goal of climate research. In view of the successful simulation of the local variability of SAT by the coupled model, we felt it worthwhile to evaluate the observed warming referring to the results from the coupled model. For this purpose, the time series of global mean SAT anomalies from the 1000-yr integration of the coupled model is compared (in Fig. 10) to the observed time series obtained during the last 110 yr. Before performing the trend analysis described below, a small linear trend of $-0.023°C\ century^{-1}$ is removed from the 1000-yr time series of the coupled model.

To assess the probability of finding a century-scale warming trend such as that observed between 1881 and 1990 in the 1000-yr time series of global mean SAT from the coupled model, Stouffer et al. (1994) calculated the probability for linear trends exceeding $0.5°C\ century^{-1}$ [i.e., the observed linear trend between 1881 and 1990 AD; Jones and Wigley (1991)]. They found that, for intervals longer than ~60 yr, there are no trends as large as $0.5°C\ century^{-1}$. In other words, the observed warming trend of $0.52°C\ century^{-1}$ is

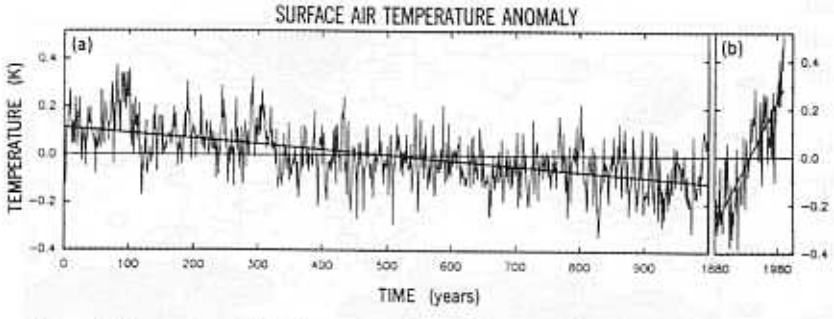

FIG. 10. Time series of globally averaged, annual mean surface air temperature anomaly from a long-term mean: (a) 1000-yr time series from the coupled ocean–atmosphere model, (b) 110-yr (1881–1990 AD) time series of observed, globally averaged temperature. The straight lines through both time series are such that the sum of squared distance between the time series and the straight line is minimized.

not found in the coupled model time series for any intervals longer than ~60 yr. Essentially similar results are obtained for the time series from the mixed layer model. In short, it is not likely that the ocean–atmosphere–land interaction in either the coupled or mixed layer model could randomly generate a substantial long-term warming trend, such as that observed since the end of the last century.

To examine spectrally the time series of global mean SAT anomaly shown in Fig. 10, the power spectra of detrended and globally averaged monthly mean SAT anomalies from the 1000-yr integrations of both coupled and mixed layer models are compared in Fig. 11 with the spectrum of detrended, observed SAT compiled by Jones and Wigley (1991). (The detrending of the observed time series reduces the contributions from fluctuations on timescales longer than 50 yr.) At multidecadal or shorter timescales, the spectra from both models are very similar to the observed spectrum, although the estimates of both models are lower than observed over the period from 1 to 10 yr [i.e., around the timescales of the Southern Oscillation, which is underestimated by the coupled model (Knutson and Manabe 1994; Knutson et al. 1997)]. At decadal to multidecadal timescales, the mixed layer model simulates the observed variability particularly well. Assuming that the model behavior is realistic, the failure of both models to reproduce the sustained, large warming trend observed during this century implies that the trend is not generated internally in the coupled system. Instead, it more likely was induced by a sustained trend in thermal forcing such as solar irradiance, atmospheric greenhouse gases, and aerosol loading.

It is notable that the global mean SAT spectra from the coupled and mixed layer models are similar to each other: the powers of both spectra increase almost monotonically with decreasing frequency. However, in both models, the spectral density of local SAT is almost white over continents and decreases very gradually with increasing frequency over oceans (Fig. 6), and it is quite different from global mean SAT spectrum described above. The difference between the spectra of local and global mean SAT suggests that, at high frequencies, SAT anomalies tend to have relatively small scales and hardly contribute to the variability of global mean SAT. On the other hand, SAT anomalies with very low frequency tend to have almost global scales, which include both oceans

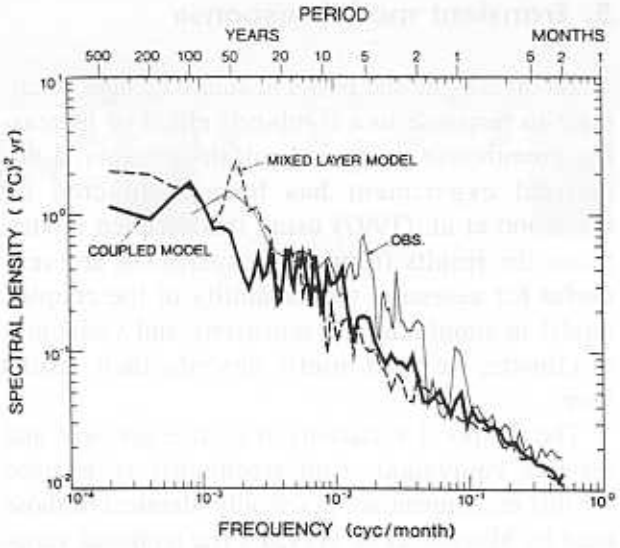

FIG. 11. Power spectra of detrended globally averaged, monthly mean SAT anomaly. The solid line represents the coupled model: the dashed line represents the mixed layer model (to detrend the time series, the least square method is used); the thin solid line represents observed [obtained by use of the data compiled by Jones and Wigley (1991)]. The spectra are the smoothed Fourier transform of autocovariance function using a Tukey window with a maximum of 2400 (200 yr) lags for the models and 480 (40 yr) lags for the observed. They are smoothed by the equally weighted averaging over the logarithmic (base 10) interval of 0.04 in frequency.

and continents, and contribute more effectively to the variability of global mean SAT. Thus, the spectral densities of global mean SAT of both coupled and mixed layer models decreases substantially with increasing frequency at interdecadal and shorter timescales despite almost white noise–like behavior of local SAT anomalies. The characteristic of the global mean SAT spectrum described above implies that the globally averaged forcing by synoptic-scale atmospheric disturbances is also substantially different from the white noise, with smaller amplitude at higher frequencies.

Although there are large and persistent anomalies of both SST and SAT near the Denmark Strait and the circumpolar ocean of the Southern Hemisphere of the coupled model, their contributions are not large enough to make the power spectrum of global mean SAT of the coupled model significantly different from that of the mixed layer model. The above discussion suggests that the thermal forcing of continental and oceanic surface by random atmospheric synoptic-scale disturbances and associated weather is essential for sustaining the decadal variability of global mean surface air temperature.

5. Transient model response

To investigate the past and future change of climate in response to a combined effect of increasing greenhouse gases and sulfate aerosols, a numerical experiment has been conducted by Haywood et al. (1997) using this coupled model. Since the results from their experiment are very useful for assessing the capability of the coupled model in simulating the sensitivity and variability of climate, we shall briefly describe their results here.

The temporal variations of sulfate aerosols and the CO_2 equivalent of all greenhouse gases used for this experiment are practically identical to those used by Mitchell et al. (1995). (The temporal variation of the CO_2 equivalent radiative forcing from 1765 to 1990 AD was based upon the 1990 Intergovernmental Panel on Climate Change report. After 1990, it was assumed to increase by 1% yr^{-1}. The direct effect of sulfate aerosols was added by increasing surface albedo at each grid box, yielding the 1990 global mean thermal forcing of ~ -0.6 W m^{-2}.) Starting from the initial condition of the 1000-yr control integration described in the preceding section, Haywood et al. performed the time integration of the coupled model over the period from 1765 to 2065 AD with thermal forcing of combined greenhouse gases and aerosols as described above.

Figure 12 illustrates the temporal variation of the globally averaged, annual mean anomalies of coupled model from 1850 to 2000 AD. For comparison, the time series of global mean surface air temperature anomaly compiled by Jones and Wigley (1991) is added to the same figure. This figure indicates that the simulated warming trend during the past 100 yr is remarkably similar to the observed trend. The model also reproduces the magnitude of the observed decadal variability reasonably well, as discussed in the preceding section.

In view of the large uncertainty in the estimation of the atmospheric loading of various aerosols and their radiative effect, the close agreement of the simulated and observed warming trends during this century could be fortuitous. The estimates of the past radiative forcing due to aerosols are also highly uncertain. In addition, many radiative forcings are neglected in this experiment; they include those due to ozone changes, other anthropogenic aerosols, indirect aerosol effects on cloud brightness, and changes in the solar irradiance. Furthermore, the climate response to these forcings is also uncertain. For example, the equilibrium response of the mixed layer model to the doubling of atmospheric CO_2 is 3.7°C, which lies in the upper half of the range of 1.5°–4.5°C estimated by the Intergovernmental Panel on Climate Change (1996). It appears significant, however, that we are unable to simulate the observed warming of the centennial timescale unless the combined effect of increasing greenhouse gases and sulfate aerosols is incorporated. This suggests that the sustained, warming trend of this century is thermally forced rather than internally generated.

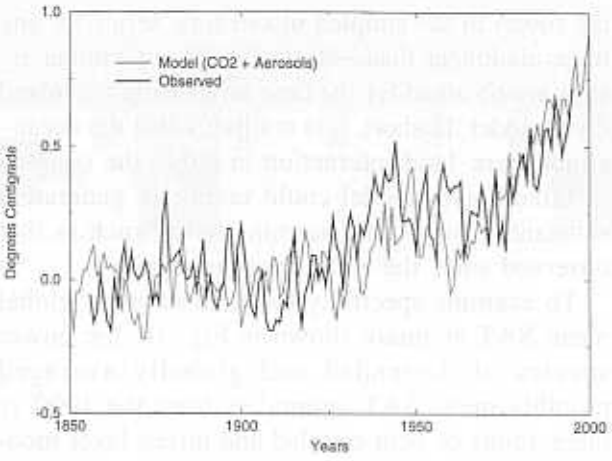

FIG. 12. Time series of globally averaged, annual mean surface air temperature anomalies (i.e., deviations from 1880–1920 mean). Thick solid line: observed (Jones et al. 1991). Thin solid line: simulated.

6. Concluding remarks

Despite its simplicity and low computational resolution, the coupled model simulates reasonably well the decadal variability of local and global mean SAT. The coupled ocean–atmosphere–land surface model has shown to be a very promising tool for the study of not only global warming but also internally generated, natural variability of climate.

Based upon the comparison between the observed and simulated variability of global mean SAT, we suggest that the sustained warming trend of this century was not generated internally through the interaction among the atmosphere, oceans and

land surface. Instead, it appears to have been forced by natural and anthropogenic thermal forcing such as that resulting from the increase of solar irradiance (Lean 1991) and greenhouse gases in the atmosphere. Similar inference could also be drawn from analysis of a global mean SAT time series obtained from the coupled model developed at the Hadley Centre of the U.K. Meteorological Office (Mitchell et al. 1995).

In addition to analyzing the time series of global mean SAT, other approaches have been employed for the detection of global warming. By comparing the pattern of the observed SAT change during the last 15–30 yr with the patterns of SAT variability generated by coupled models, Hegerl et al. (1996) concluded that statistically significant, externally induced warming has been observed. Santer et al. (1996) noted that the observed patterns of temperature change in free atmosphere from 1963 to 1997 are similar to those obtained by climate models that incorporate various combinations of changes in carbon dioxide, anthropogenic sulfate aerosols, and stratospheric ozone concentrations. The conclusions of the studies mentioned above are clearly in support of the recent statement of the Intergovernmental Panel on Climate Change (1996): "The balance of evidence suggests a discernible human influence on global climate."

Acknowledgments. We thank A.J. Broccoli, T.R. Knutson, and J.D. Mahlman for reviewing the manuscript and providing us with many valuable comments.

References

Delworth, T. L., S. Manabe, and R. J. Stouffer, 1993: Interdecadal variations of the thermohaline circulation in a coupled ocean-atmosphere model. *J. Climate,* **6,** 1993–2011.

——, ——, and ——, 1997: Multidecadal climate variability in the Greenland Sea and surrounding regions: A coupled model simulation. *Geophys. Res. Lett.*, **24,** 257–260.

Hall, A., and S. Manabe, 1997: Can local linear stochastic theory explain sea surface temperature and salinity variability? *Climate Dynamics,* **13,** 167–180.

Hasselmann, K., 1976: Stochastic climate models. Part I: Theory. *Tellus,* **28,** 473–485.

Haywood, J., R. J. Stouffer, R. T. Wetherald, S. Manabe, and V. Ramaswamy, 1997: Transient response of a coupled model to estimated changes in greenhouse gas and sulfate concentrations. *Geophys. Res. Lett.*, **24,** 1335–1338.

Hegerl, G. C., H. von Storch, K. Hasselmann, B. D. Santer, U. Cubasch, and P. D. Jones, 1996: Detecting greenhouse-gas-induced climate change with an optimum fingerprint method. *J. Climate,* **9,** 2281–2306.

Intergovernmental Panel on Climate Change, 1996: *Climate Change 1995: The Science of Climate Change.* Cambridge University Press, 572 pp.

Jones, P., and T. M. L. Wigley, 1991: *Global and Hemispheric Anomalies. Trend '91: A Compendium of Data on Global Change.* T. A. Boden, R. J. Sepanski, and F. W. Stoss, Eds., Oak Ridge National Laboratory, 512–517.

Knutson, T. R., and S. Manabe, 1994: Impact of increased CO_2 on simulated ENSO-like phenomena. *Geophys. Res. Lett.*, **21,** 2295–2298.

——, ——, and D. Gu, 1997: Simulated ENSO in a global coupled ocean–atmosphere model: Multidecadal amplitude modulation and CO_2 sensitivity. *J. Climate,* **10,** 138–161.

Lean, J., 1991: Variation in the sun's radiative output. *Rev. Geophys.*, **29,** 505–535.

Manabe, S., and R. J. Stouffer, 1988: Two stable equilibria of a coupled ocean–atmosphere model. *J. Climate,* **1,** 841–866.

——, and ——, 1996: Low frequency variability of surface air temperature in a 1000-yr integration of a coupled atmosphere–ocean–land surface model. *J. Climate,* **9,** 376–393.

Mitchell, J. F. B., T. C. Johns, J. M. Gregory, and S. F. B. Tett, 1995: Climate response to increasing level of greenhouse gases and sulphate aerosols. *Nature,* **376,** 501–504.

Santer, B. D., and Coauthors, 1996: A search for human influences on the thermal structure of the atmosphere. *Nature,* **382,** 39–46.

Stouffer, R. J., S. Manabe, and K. Ya. Vinnikov, 1994: Model assessment of the role of natural variability in recent global warming. *Nature,* **367,** 634–636.